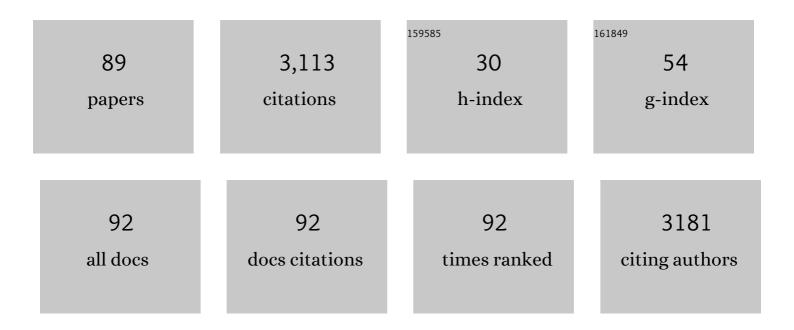
## Nikolaos Papanikolaou

List of Publications by Year in descending order

Source: https://exaly.com/author-pdf/8759583/publications.pdf Version: 2024-02-01



#	Article	IF	CITATIONS
1	Radiomics/Radiogenomics in Lung Cancer: Basic Principles and Initial Clinical Results. Cancers, 2022, 14, 1657.	3.7	15
2	Comparison of MRI Features of Fat Fraction and ADC for Early Treatment Response Assessment in Participants with Multiple Myeloma. Radiology, 2022, 304, 137-144.	7.3	18
3	Machine learning in predicting extracapsular extension (ECE) of prostate cancer with MRI: a protocol for a systematic literature review. BMJ Open, 2022, 12, e052342.	1.9	1
4	Discrimination of Tumor Texture Based on MRI Radiomic Features: Is There a Volume Threshold? A Phantom Study. Applied Sciences (Switzerland), 2022, 12, 5465.	2.5	2
5	A multicenter study on radiomic features from T 2 â€weighted images of a customized MR pelvic phantom setting the basis for robust radiomic models in clinics. Magnetic Resonance in Medicine, 2021, 85, 1713-1726.	3.0	22
6	Improving performance and generalizability in radiogenomics: a pilot study for prediction of IDH1/2 mutation status in gliomas with multicentric data. Journal of Medical Imaging, 2021, 8, 031905.	1.5	5
7	Breast cancer surgery with augmented reality. Breast, 2021, 56, 14-17.	2.2	34
8	Radiomics in Oncology: A Practical Guide. Radiographics, 2021, 41, 1717-1732.	3.3	139
9	Diffusion-weighted imaging and texture analysis: current role for diffuse liver disease. Abdominal Radiology, 2020, 45, 3523-3531.	2.1	9
10	UniProt-Related Documents (UniReD): assisting wet lab biologists in their quest on finding novel counterparts in a protein network. NAR Genomics and Bioinformatics, 2020, 2, Iqaa005.	3.2	8
11	CT-Based Radiomics Analysis to Predict Malignancy in Patients with Intraductal Papillary Mucinous Neoplasm (IPMN) of the Pancreas. Cancers, 2020, 12, 3089.	3.7	32
12	New boundaries of liver imaging: from morphology to function. European Journal of Internal Medicine, 2020, 79, 12-22.	2.2	2
13	Quantification of tumor burden in multiple myeloma by atlas-based semi-automatic segmentation of WB-DWI. Cancer Imaging, 2020, 20, 6.	2.8	16
14	How to develop a meaningful radiomic signature for clinical use in oncologic patients. Cancer Imaging, 2020, 20, 33.	2.8	110
15	Interpretable artificial intelligence framework for COVID†19 screening on chest X†rays. Experimental and Therapeutic Medicine, 2020, 20, 727-735.	1.8	85
16	Advancing Covid‑19 differentiation with a robust preprocessing and integration of multi‑institutional open‑repository computer tomography datasets for deep learning analysis. Experimental and Therapeutic Medicine, 2020, 20, 1-1.	1.8	10
17	Artificial intelligence radiogenomics for advancing precision and effectiveness in oncologic care (Review). International Journal of Oncology, 2020, 57, 43-53.	3.3	49
18	Diffusion tensor-based fiber tracking of the male urethral sphincter complex in patients undergoing radical prostatectomy: a feasibility study. Insights Into Imaging, 2020, 11, 126.	3.4	0

#	Article	IF	CITATIONS
19	Perfusion Magnetic Resonance as a Biomarker for Sorafenib-Treated Advanced Hepatocellular Carcinoma: A Pilot Study. GE Portuguese Journal of Gastroenterology, 2019, 26, 260-267.	0.8	4
20	Sparse Representations on DW-MRI: A Study on Pancreas. , 2019, , .		0
21	Challenges and Promises of Radiomics for Rectal Cancer. Current Colorectal Cancer Reports, 2019, 15, 175-180.	0.5	6
22	Automatic Detection and Segmentation of Lung Lesions using Deep Residual CNNs. , 2019, , .		4
23	Functional and molecular MRI of the bone marrow in multiple myeloma. British Journal of Radiology, 2018, 91, 20170389.	2.2	25
24	Correlation between quantitative and semiquantitative parameters in DCE-MRI with a blood pool agent in rectal cancer: can semiquantitative parameters be used as a surrogate for quantitative parameters?. Abdominal Radiology, 2017, 42, 1342-1349.	2.1	14
25	Thin isotropic FLAIR MR images at 1.5T increase the yield of focal cortical dysplasia transmantle sign detection in frontal lobe epilepsy. Epilepsy Research, 2017, 132, 1-7.	1.6	14
26	Diffusion weighted imaging in patients with rectal cancer: Comparison between Gaussian and non-Gaussian models. PLoS ONE, 2017, 12, e0184197.	2.5	6
27	Apparent Diffusion Coefficient Quantification in Determining the Histological Diagnosis of Malignant Liver Lesions. Journal of Cancer, 2016, 7, 730-735.	2.5	14
28	Addressing Intravoxel Incoherent Motion challenges through an optimized fitting framework for quantification of perfusion. , 2016, , .		0
29	Fiber tracking: A qualitative and quantitative comparison between four different software tools on the reconstruction of major white matter tracts. European Journal of Radiology Open, 2016, 3, 153-161.	1.6	49
30	Diffusion-weighted MR imaging of pancreatic cancer: A comparison of mono-exponential, bi-exponential and non-Gaussian kurtosis models. European Journal of Radiology Open, 2016, 3, 79-85.	1.6	27
31	Evidence for APOBEC3B mRNA and protein expression in oral squamous cell carcinomas. Experimental and Molecular Pathology, 2016, 101, 314-319.	2.1	10
32	Visualizing tumor environment with perfusion and diffusion MRI. , 2016, , .		2
33	Prognostic value of preoperative dynamic contrast-enhanced MRI perfusion parameters for high-grade glioma patients. Neuroradiology, 2016, 58, 1197-1208.	2.2	45
34	Diffusion Modelling Tool (DMT) for the analysis of Diffusion Weighted Imaging (DWI) Magnetic Resonance Imaging (MRI) data. , 2016, , .		7
35	Thrombocytopenia in critically ill patients with severe sepsis/septic shock: Prognostic value and association with a distinct serum cytokine profile. Journal of Critical Care, 2016, 32, 9-15.	2.2	50
36	Role of Magnetic Resonance Imaging in Primary Rectal Cancer—Standard Protocol and Beyond. Seminars in Ultrasound, CT and MRI, 2016, 37, 323-330.	1.5	8

#	Article	IF	CITATIONS
37	Automated and Semiautomated Segmentation of Rectal Tumor Volumes on Diffusion-Weighted MRI: Can It Replace Manual Volumetry?. International Journal of Radiation Oncology Biology Physics, 2016, 94, 824-831.	0.8	50
38	Magnetization transfer imaging to assess tumour response after chemoradiotherapy in rectal cancer. European Radiology, 2016, 26, 390-397.	4.5	13
39	Whole-liver diffusion-weighted MRI histogram analysis. European Journal of Gastroenterology and Hepatology, 2015, 27, 399-404.	1.6	10
40	Magnetization Transfer Ratio. Investigative Radiology, 2014, 49, 29-34.	6.2	30
41	A software prototype for the assessment of tumor treatment response using diffusion and perfusion MR imaging. , 2012, 2012, 388-91.		1
42	Comparison between two-point and four-point methods for quantification of apparent diffusion coefficient of normal liver parenchyma and focal lesions. Value of normalization with spleen. European Journal of Radiology, 2010, 73, 305-309.	2.6	51
43	Crohn's disease lymphadenopathy: MR imaging findings. European Journal of Radiology, 2009, 69, 425-428.	2.6	45
44	Respiratory gated diffusion-weighted imaging of the liver: value of apparent diffusion coefficient measurements in the differentiation between most commonly encountered benign and malignant focal liver lesions. European Radiology, 2008, 18, 486-492.	4.5	220
45	Preoperative Imaging Staging of Rectal Cancer. Digestive Diseases, 2007, 25, 20-32.	1.9	35
46	Myocardial and liver iron status using a fastT2* quantitative MRI (T2*qMRI) technique. Magnetic Resonance in Medicine, 2007, 57, 742-753.	3.0	34
47	Experimental determination of the effect of detector size on profile measurements in narrow photon beams. Medical Physics, 2006, 33, 3700-3710.	3.0	64
48	3D polymer gel dosimetry using a 3D (DESS) and a 2D MultiEcho SE (MESE) sequence. Journal of Physics: Conference Series, 2006, 56, 259-262.	0.4	0
49	Use of polymer gel dosimetry for the determination of the detector size effect on profile measurements of a 5 mm diameter photon beam. Journal of Physics: Conference Series, 2006, 56, 245-248.	0.4	1
50	Fractional anisotropy and mean diffusivity measurements on normal human brain: comparison between low- and high-resolution diffusion tensor imaging sequences. European Radiology, 2006, 16, 187-192.	4.5	35
51	Imaging of small intestinal Crohn's disease: comparison between MR enteroclysis and conventional enteroclysis. European Radiology, 2006, 16, 1915-1925.	4.5	150
52	Magnetic resonance imaging evaluation of small intestinal Crohn's disease. Bailliere's Best Practice and Research in Clinical Gastroenterology, 2006, 20, 137-156.	2.4	72
53	Dark Lumen MR Colonography: Can High Spatial Resolution VIBE Imaging Improve the Detection ofÂColorectal Masses?. RoFo Fortschritte Auf Dem Gebiet Der Rontgenstrahlen Und Der Bildgebenden Verfahren, 2006, 178, 1073-1078.	1.3	4
54	Complementary role of helical CT cholangiography to MR cholangiography in the evaluation of biliary function and kinetics. European Radiology, 2005, 15, 2130-2139.	4.5	14

#	Article	IF	CITATIONS
55	Quantification of magnetization transfer rate and native T1 relaxation time of the brain: correlation with magnetization transfer ratio measurements in patients with multiple sclerosis. Neuroradiology, 2005, 47, 189-196.	2.2	30
56	Magnetic Resonance Enteroclysis. Seminars in Ultrasound, CT and MRI, 2005, 26, 237-246.	1.5	39
57	T2 relaxation time analysis in patients with multiple sclerosis: correlation with magnetization transfer ratio. European Radiology, 2004, 14, 115-122.	4.5	47
58	Assessment of Crohn?s disease activity in the small bowel with MR and conventional enteroclysis: preliminary results. European Radiology, 2004, 14, 1017-1024.	4.5	172
59	Real-time high-resolution MRI for the assessment of gastric motility: Pre- and postpharmacological stimuli. Journal of Magnetic Resonance Imaging, 2004, 19, 453-458.	3.4	35
60	Real time high resolution magnetic resonance imaging for the assessment of gastric motility disorders. Gut, 2004, 53, 1256-1261.	12.1	108
61	MR colonography with fecal tagging: comparison between 2D turbo FLASH and 3D FLASH sequences. European Radiology, 2003, 13, 448-452.	4.5	21
62	Detection of malignant bone marrow involvement with dynamic contrast-enhanced magnetic resonance imaging. Annals of Oncology, 2003, 14, 152-158.	1.2	58
63	Transtympanic Iontophoresis with a Biocompatible Paramagnetic Solution at MR Imaging: Experimental Feasibility Study in Rabbits. Radiology, 2002, 223, 689-694.	7.3	1
64	Biexponential T2 Relaxation Time Analysis of the Brain. Investigative Radiology, 2002, 37, 363-367.	6.2	24
65	Technical Challenges and Clinical Applications of Magnetic Resonance Enteroclysis. Topics in Magnetic Resonance Imaging, 2002, 13, 397-408.	1.2	20
66	Optimization of a contrast medium suitable for conventional enteroclysis, MR enteroclysis, and virtual MR enteroscopy. Abdominal Imaging, 2002, 27, 517-522.	2.0	27
67	Development of contrast-enhanced virtual MR cholangioscopy: a feasibility study. European Radiology, 2002, 12, 1438-1441.	4.5	14
68	Hepatic involvement in hereditary hemorrhagic telangiectasia (Rendu-Osler-Weber disease). European Radiology, 2002, 12, S51-S55.	4.5	23
69	MR enteroclysis: technical considerations and clinical applications. European Radiology, 2002, 12, 2651-2658.	4.5	156
70	Contrast-Enhanced Magnetic Resonance Cholangiography Versus Heavily T2-Weighted Magnetic Resonance Cholangiography. Investigative Radiology, 2001, 36, 682-686.	6.2	38
71	Increased signal intensity on fat-suppressed three-dimensional T1-weighted pulse sequences in patellar tendon: magic angle effect?. Skeletal Radiology, 2001, 30, 67-71.	2.0	21
72	T2-weighted magnetic resonance imaging of the liver: comparison of fat-suppressed GRASE with conventional spin echo, fat-suppressed turbo spin echo, and gradient echo at 1.0 T. Abdominal Imaging, 2001, 26, 139-145.	2.0	6

#	Article	IF	CITATIONS
73	MR enteroclysis protocol optimization: comparison between 3D FLASH with fat saturation after intravenous gadolinium injection and true FISP sequences. European Radiology, 2001, 11, 908-913.	4.5	98
74	MR Enteroclysis Imaging of Crohn Disease. Radiographics, 2001, 21, S161-S172.	3.3	183
75	Deformity of the Superior Mesenteric Vein. American Journal of Roentgenology, 2001, 176, 1600-1601.	2.2	0
76	MR Imaging of the Small Bowel with a True-FISP Sequence After Enteroclysis with Water Solution. Investigative Radiology, 2000, 35, 707-711.	6.2	87
77	Comparison of dual spin echo echo planar imaging (SE_EPI), turbo spin echo with fat suppression and conventional dual spin echo sequences for T2-weighted MR imaging of focal liver lesions. Magnetic Resonance Imaging, 2000, 18, 715-719.	1.8	10
78	Comparison of echo planar imaging, gradient echo and fast spin echo MR scans of knee menisci. Computerized Medical Imaging and Graphics, 2000, 24, 309-316.	5.8	6
79	Single-shot turbo spin-echo MR myelography: comparison with 3D-turbo spin-echo MR myelography and T2-turbo spin-echo at 1T. Computerized Medical Imaging and Graphics, 2000, 24, 37-42.	5.8	4
80	Blueberry juice used per os in upper abdominal MR imaging: composition and initial clinical data. European Radiology, 2000, 10, 909-913.	4.5	56
81	Non-invasive myocardial iron assessment in thalassaemic patients: T2 relaxometry and magnetization transfer ratio measurements. Acta Radiologica, 2000, 41, 348-351.	1.1	28
82	MR Cholangiopancreatography Before and After Oral Blueberry Juice Administration. Journal of Computer Assisted Tomography, 2000, 24, 229-234.	0.9	52
83	MR Imaging of the Liver Using an Ultrafast 3D Multi-Shot EPI Sequence. Acta Radiologica, 1999, 40, 322-325.	1.1	2
84	Comparison of T1-weighted spin-echo and 3D T1-weighted multi-shot echo planar pulse sequences in imaging the brain at IT. Magnetic Resonance Imaging, 1999, 17, 663-668.	1.8	3
85	Magnetic resonance cholangiopancreatography: Comparison between respiratory-triggered turbo spin echo and breath hold single-shot turbo spin echo sequences. Magnetic Resonance Imaging, 1999, 17, 1255-1260.	1.8	23
86	MR cholangiopancreatography at 0.5 T with a 3D inversion recovery turbo-spin-echo sequence. European Radiology, 1997, 7, 1318-1322.	4.5	4
87	Acute subarachnoid haemorrhage: detection with magnetic resonance imaging. British Journal of Radiology, 1996, 69, 601-609.	2.2	22
88	Bone marrow lesions: evaluation with fat-suppression turbo spin echo MR imaging at 0.5 T. European Radiology, 1996, 6, 895-9.	4.5	2
89	Cyclopia and exadactyly: CT and MRI findings. Dentomaxillofacial Radiology, 0, 28, 372-374.	2.7	0